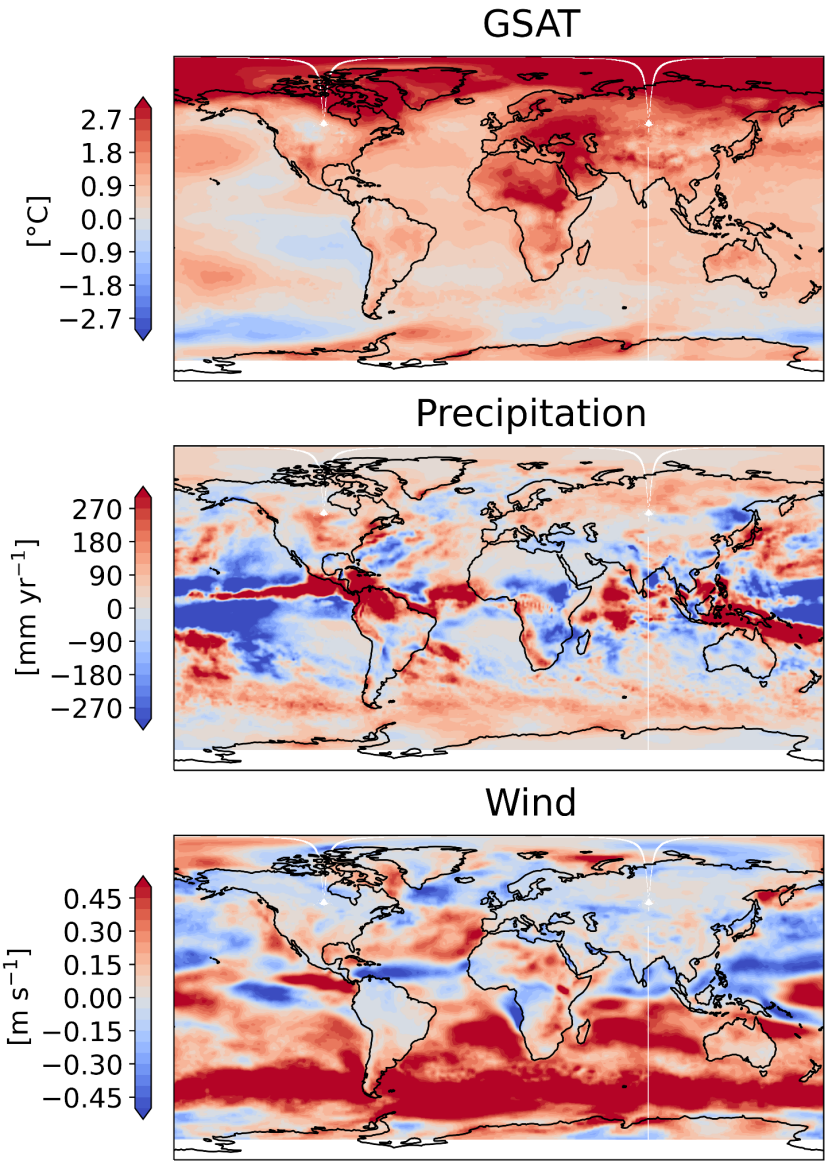

Supplement Figure S1. Spatial distribution of 1980-2022 changes in major atmospheric variables. Changes in global surface atmospheric temperature (GSAT), precipitation and wind speed change over 1980-2022 derived from linear trends using the ERA-20C (1900-2010) product, and extended with ERA5 (2011-2022) reanalysis product.

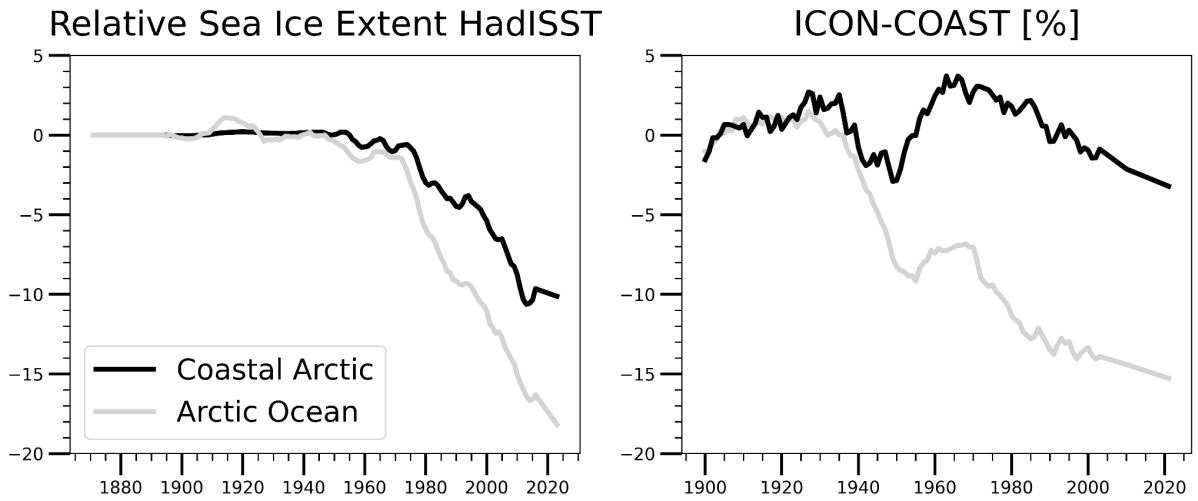

Supplement Figure S2. Modelled and observed evolution of coastal and open water Arctic sea ice. Relative changes in Arctic coastal and open water sea ice extent based on the observational dataset HadISST and the model ICON-COAST.

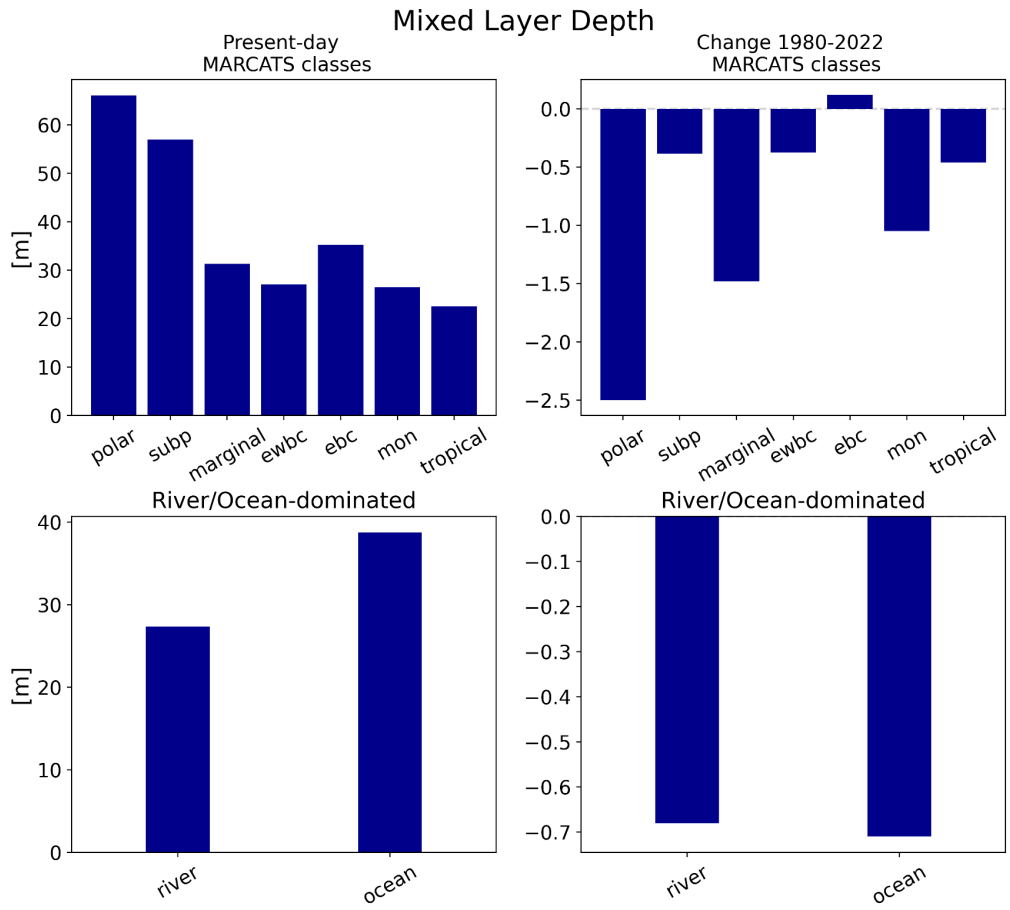

Supplement Figure S3. Present day mixed layer depths and their 1980-2022 changes for different coastal classes. Panel a and b shows simulated present-day (2000-2022 average) mean surface temperature and their 1980-2022 change for major high-level MARCATS coastal classes derived from linear trend: eastern boundary current (ebc), western boundary current (ewbc), monsoonal (mon), subpolar (subp), polar, marginal and tropical as defined in Laruelle et al. (2013) based on catchment properties. Panel c and d show the same variables for defined river/ocean-dominated shelves. We thereby computed means from ICON-COAST and HAMOCC-RIVER.

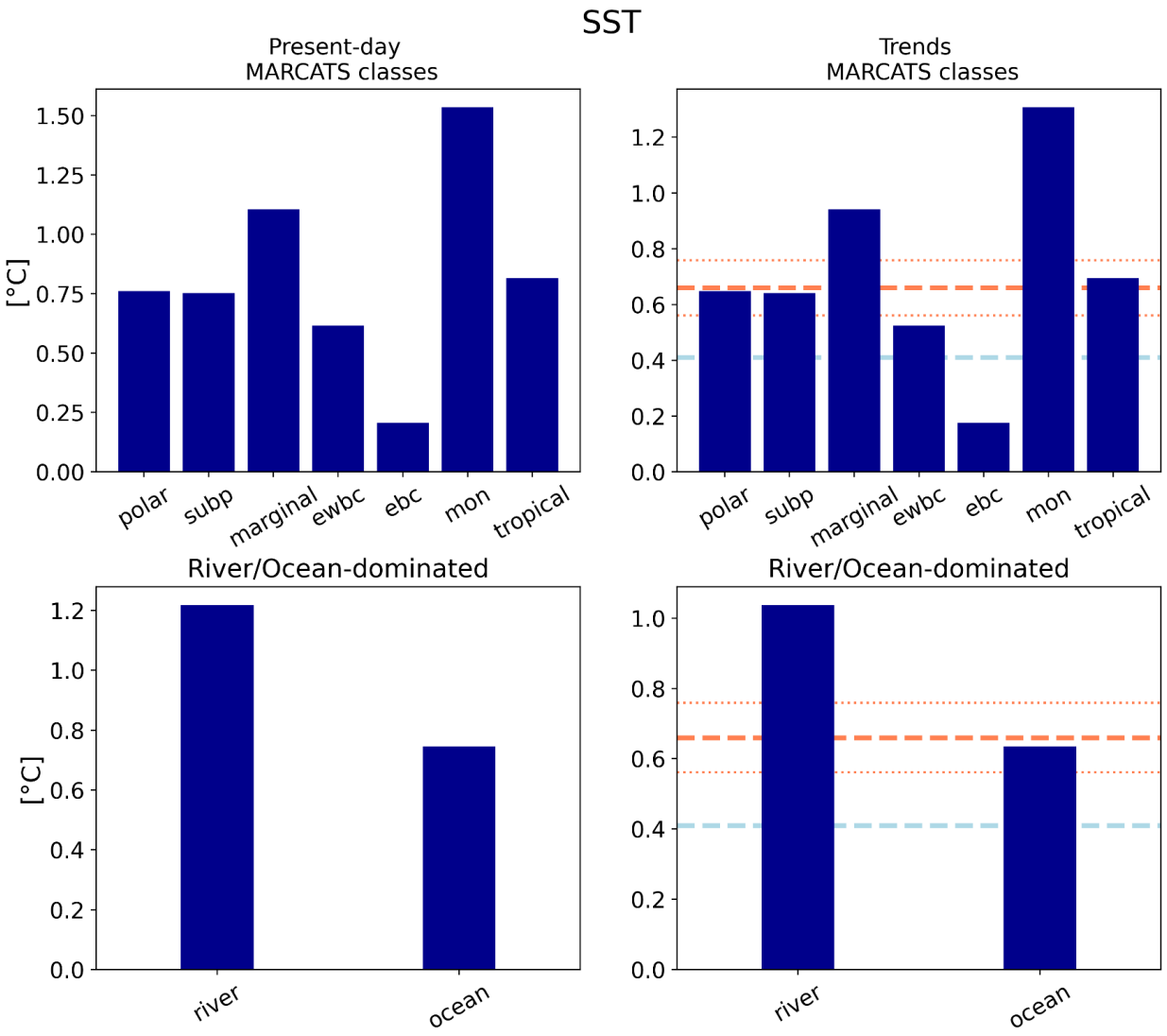

Supplement Figure S4. Present day SST and their 1980-2022 changes in different coastal classes. Panel a and b shows simulated present-day (2010-2020 average) mean surface temperature and their 1980-2022 change for major high-level MARCATS coastal classes: eastern boundary current (ebc), western boundary current (ewbc), monsoonal (mon), subpolar (subp), polar, marginal and tropical as defined in Laruelle et al. (2013) based on catchment properties. Panel c and d show the same variables for defined river/open ocean-dominated shelves. We thereby computed the mean from ICON-COAST and HAMOCC. Red dashed lines show coastal ocean means, dotted lines the 15% deviations from the coastal ocean means, and dashed blue the open ocean mean.

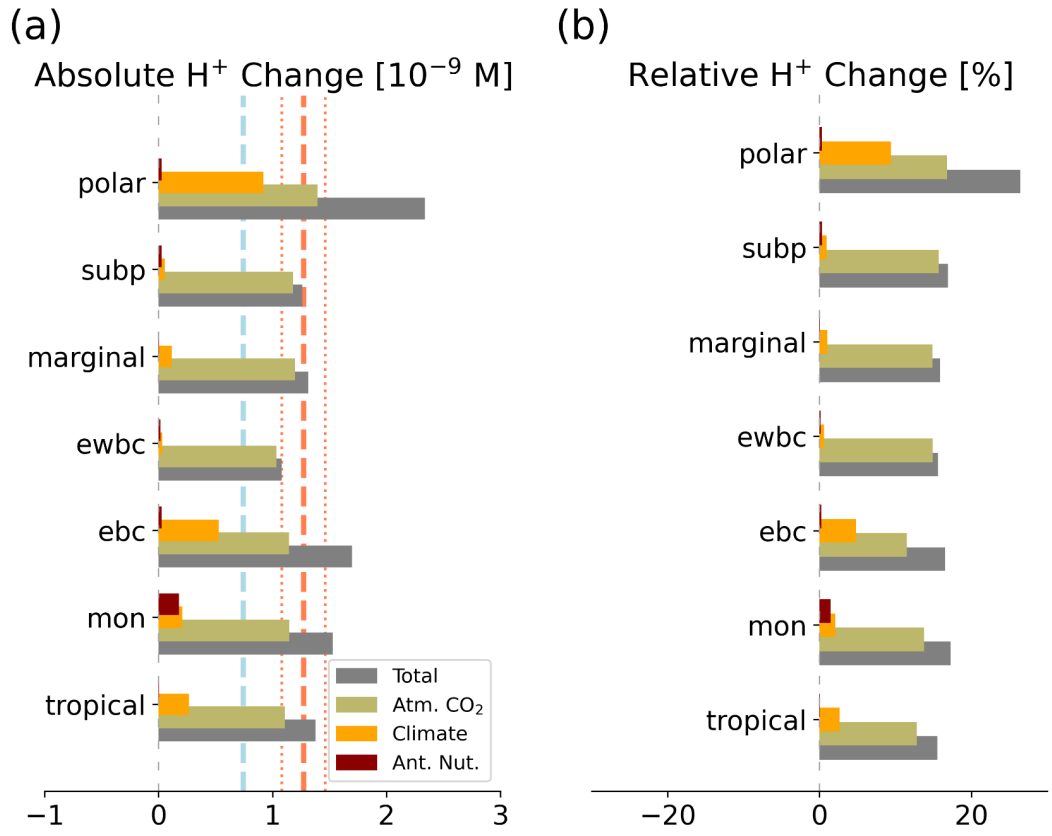

Supplement Figure S5. Absolute (panel a) and relative (panel b) total changes in H^+ over 1980-2022. We show total 1980-2022 changes and those driven by climate and anthropogenic nutrients (Ant. Nut.) perturbations for the major high-level MARCATS coastal classes derived from linear trend: eastern boundary current (ebc), western boundary current (ewbc), monsoonal (mon), subpolar (subp), polar, marginal and tropical. Red dashed lines show coastal ocean

means, dotted lines the 15% deviations from the coastal ocean means, and dashed blue the open ocean mean.

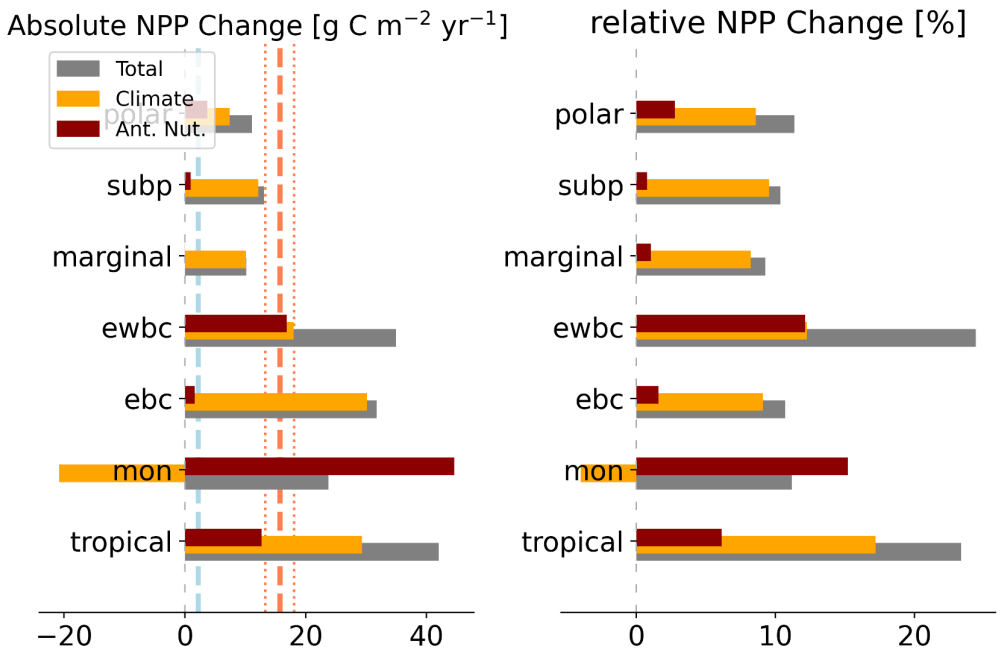

Supplement Figure S6. Absolute (panel a) and relative (panel b) total changes in NPP over 1980-2022. We show total changes, as well as those only driven by climate and anthropogenic nutrients (Ant. Nut.) perturbations for the major high-level MARCATS coastal classes derived from linear trend: eastern boundary current (ebc), western boundary current (ewbc), monsoonal (mon), subpolar (subp), polar, marginal and tropical. Red dashed lines show coastal ocean means, dotted lines the 15% deviations from the coastal ocean means, and dashed blue the open ocean mean.

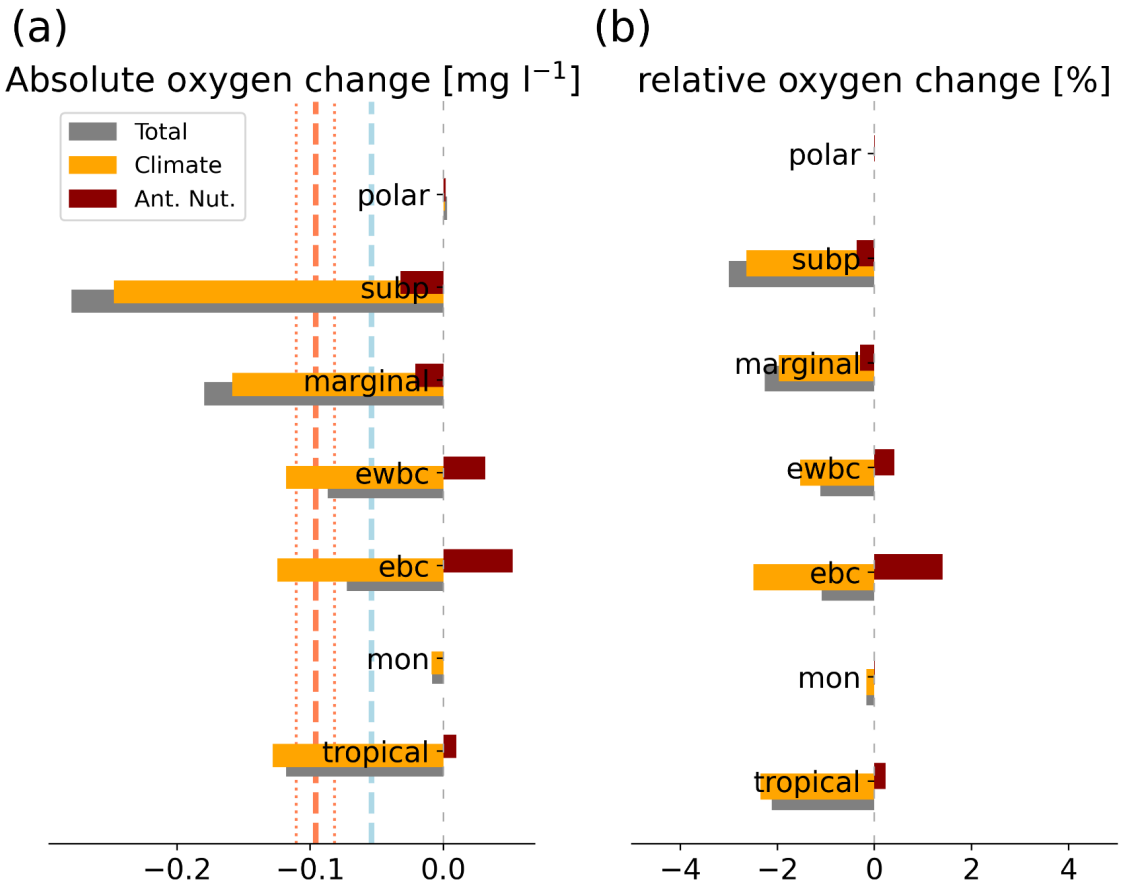

Supplement Figure S7. Absolute (panel a) and relative changes (panel b) in O_2 over 1980-2022. We show total 1980-2022 changes, as well as those driven by climate and river-induced perturbations for the major high-level MARCATS coastal classes derived from linear trend: eastern boundary current (ebc), western boundary current (ewbc), monsoonal (mon), subpolar (subp), polar, marginal and tropical. Red dashed lines show coastal ocean means, dotted lines the 15% deviations from the coastal ocean means, and dashed blue the open ocean mean.

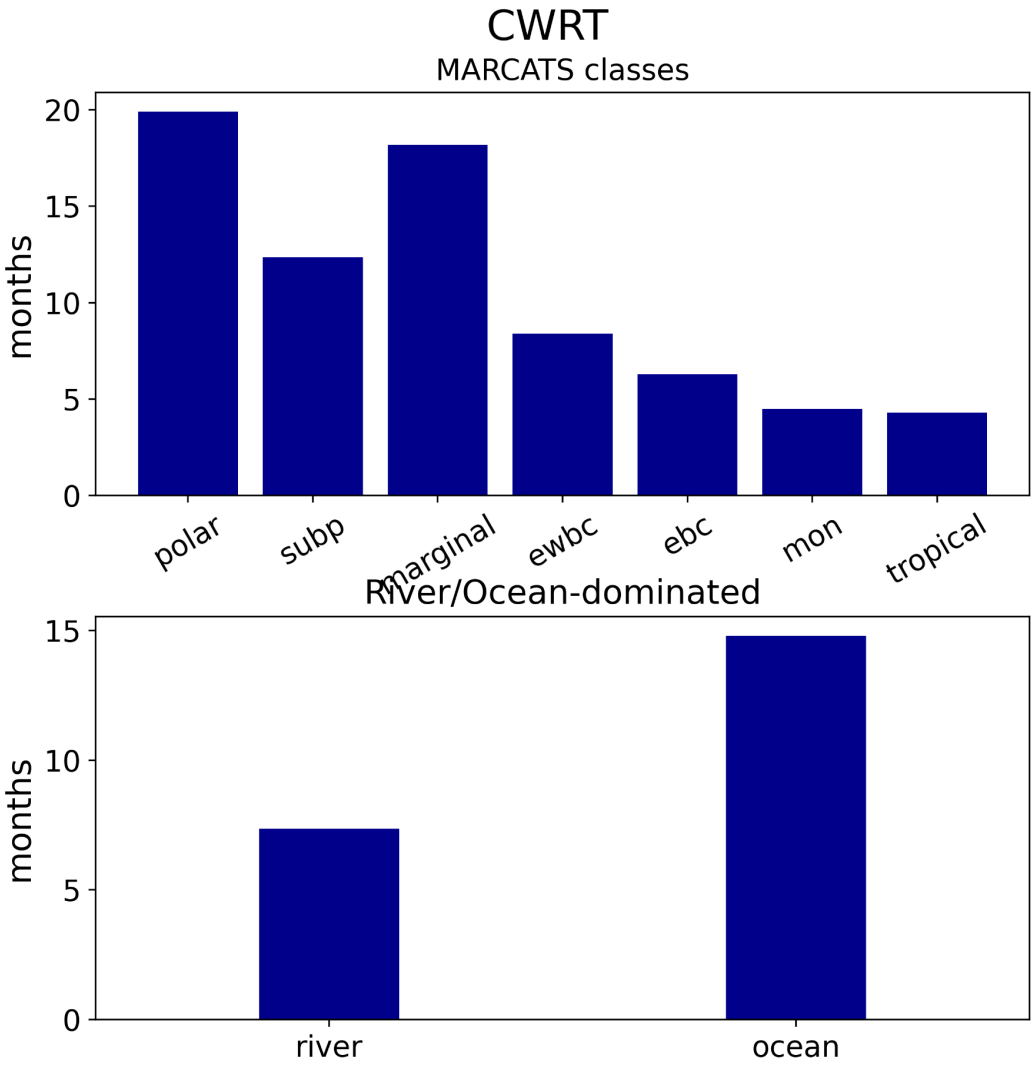

Supplement Figure S8. **Coastal water residence times (CWRTs) for coastal ocean classes.** Simulated CWRTs for major high-level MARCATS coastal classes: eastern boundary current (ebc), western boundary current (ewbc), monsoonal (mon), subpolar (subp), polar, marginal and tropical as defined in Laruelle et al. (2013) based on catchment properties. Panel c and d show the same variables for defined river/open ocean-dominated shelves. We thereby computed these from inert tracer HAMOCC simulations (Lacroix et al., 2021).